Ultrasonics Sonochemistry 21 (2014) 1641–1648

Contents lists available at ScienceDirect

Ultrasonics Sonochemistry

journal homepage: www.elsevier.com/locate/ultson

Preparation and characterization of conductive nanostructured particles based on polyaniline and cellulose nanofibers

U.M. Casado, M.I. Aranguren, N.E. Marcovich *

Institute of Materials Science and Technology (INTEMA), National University of Mar del Plata – National Research Council (CONICET), Av. Juan B. Justo 4302, 7600 Mar del Plata, Argentina

ARTICLE INFO

Article history:
Received 11 September 2013
Received in revised form 12 March 2014
Accepted 13 March 2014
Available online 21 March 2014

Keywords:
Polyaniline
Nanocellulose
Conductive nanoparticles
Stable suspensions

ABSTRACT

Conducting polyaniline (PANI) and cellulose coated PANI (PANI-NC) nanostructures with sizes of about 80–100 nm, doped with hydrochloric acid were synthesized by a sonochemical method. Both type of particles resulted electrically conductive (direct current conductivity of 0.059 and 0.075 S/cm for PANI and PANI-NC structures, respectively) and could be dispersed easily in water, leading to green colored suspensions that remain stable for more than 4 h. The morphology, crystallinity, electrical conductivity (σ) and thermal stability of the obtained PANI based structures were investigated and compared. Furthermore, UV–Vis spectroscopy and rheology of water suspensions were used to explain the measured properties. Although the concentration of cellulose fibers used to synthesize the PANI-NC structures was very low, important differences respect to the neat PANI fibers regarding the microstructure, electrical conductivity and suspension behavior were found.

1. Introduction

The controlled synthesis of nanometer-scale materials is a fascinating objective in modern material science. Recently, much attention has been paid to the synthesis of micro/nanostructured conducting polymers for their unique properties and promising potential applications in nanodevices [1–3]. Among the conducting nanostructured polymers, polyaniline (PANI) nanostructures have received much attention for their applications in novel optoelectronic devices, sensors and actuators, and conducting polymer composites [4–6] because of their low cost, ease of preparation, environmental stability, and reversible acid/base doping/dedoping characteristics [7]. PANI nanostructures, including nanowires, nanorods, nanotubes and nanofibers (NFs), have shown superior performance over other forms of the polymer [8]. Among their many advantages, the large interfacial area between PANI nanostructures and their surrounding [5] improves the dispersibility in the hosting matrices. Various strategies, including template synthesis, self-assembly, electrospinning, electrochemical methods, rapid mixing polymerization, sonochemical synthesis and interfacial polymerization have been developed for the synthesis of PANI nanofibers and nanotubes [9,10].

In recent years, it has been investigated the possibility of PANI coatings on fillers like clay, silica, silicates, carbon black, poly(methyl methacrylate) [11,12]. In particular, PANI was polymerized in the presence of $BaTiO_3$ nanoparticles to produce nanohybrid conductors [13], as well as SnO_2 nanoparticles to produce gas sensors [14], and Ag_2Te to produce core–shell nanoparticles [15]. Also, PANI-Ag hybrid has attracted considerable interest because of its potential in technological applications in the field of the electronic industry: transducers, actuators, sensors, batteries and biomaterials [16,17]. PANI has poor mechanical properties, but it is possible to improve and modify it through the incorporation of micro and nanosized particles. However, there are very few papers that report the utilization of PANI as the polymeric matrix and nano-/microsized fillers as reinforcement for improving mechanical properties [12]. Cellulose is one of the most abundant materials in nature; it can be extracted from different plants and it is naturally present as ordered and well-packed aggregates of nanofibrils. Cellulose nanofibrils possess several advantages such as low cost, low density, non-toxicity, renewable nature, biodegradability, capability of forming stable aqueous suspensions and remarkable mechanical properties that allows improving the mechanical performance of polymers at quite low fiber concentrations [6,18,19]. Thus, carrying out the polymerization of aniline in presence of nanocellulose fibers seems to be an obvious alternative to prepare conductive particles with improved mechanical properties. In fact, the existent literature demonstrates these hybrid particles present several benefits, as compared with neat PANI structures. Mattoso et al. [20] prepared polyaniline coated cellulose by in situ polymerization of aniline onto "never-dried" nano

* Corresponding author. Tel.: +54 223 481 6600; fax: +54 223 481 0046.
E-mail address: marcovic@fi.mdp.edu.ar (N.E. Marcovich).

http://dx.doi.org/10.1016/j.ultsonch.2014.03.012
1350-4177/

cellulose fibers and demonstrated that the resulting aqueous suspensions were much more stable than PANI ones and thus, shining films with interesting electrical conductivities were obtained. Casado et al. [6] found that PANI-NC fibers resulted more conductive than neat PANI ones and the same behavior was found for the resulting shape memory composite films. Li et al. [21] prepared PANI-coated conductive paper by in situ polymerization of aniline, indicating that the pulp fibers promoted the dispersion of the PANI particles generated, preventing their aggregation in the reaction system, which was favorable for the doping of PANI with *p*-toluenesulfonic acid. However, these research works were focused on the final composite or conductive paper and thus, the relationship structure–properties of the neat and hybrid PANI particles was not systematically studied. Thus, the main goal of this work is to obtain and characterize hybrid particles with similar or higher conductivity than that of PANI using nanocellulose fibersas nucleating/reactive particles during the sonochemical synthesis.

2. Experimental

2.1. Preparation of cellulose nanofibers

Aqueous suspensions of cellulose crystals were prepared from commercial microcrystalline cellulose (Aldrich, cat. No. 31,069-7) by acid hydrolysis, using an optimized procedure [18]. The microcrystalline cellulose was mixed with aqueous sulfuric acid (64 wt%) in a ratio of microcrystalline cellulose to acid of 1:8.75 g/ml. The mixture was then held at 45 °C for 0.5 h under strong stirring. The resulting suspension was diluted with an equal volume of water and dialyzed using a cellulose dialysis membrane (Spectra/Por 2, SpectrumLabs, Unitek de Argentina, molecular weight cut off = 12–14,000 daltons) to pH = 5–6 to eliminate the excess of acid. The final suspension was stabilized by ultrasonic treatment (0.5 h, Elmasonic P 60H, Elma). The concentration of this suspension was determined by drying aliquots of known volume and determining the fiber weight.

2.2. Synthesis of PANI and PANI-cellulose nanofibers

PANI fibers were synthesized by the sonochemical method proposed by Jing et al. [10] and adapted with small modifications. Aniline (ANI, Carlo Erba) was doubly distilled in presence of zinc powders. Ammonium persulfate (APS, Anedra, RA-ACS-) and hydrochloric acid (HCl, 36–37 wt%, Anedra, RA-ACS) were used as received. In a typical procedure, a 0.2 mol/L solution of ANI in aqueous HCl (1 mol/L) was prepared in a beaker and sonicated by placing the beaker in an ultrasonic cleaning bath (Elmasonic P 60H, Elma), using a power of 160 W and operated at 37 kHz. Then, 0.2 mol of APS were dissolved in 100 ml HCl (1 mol/L) and dropwise added to the ANI containing beaker, which was kept at 25 °C during the 4 h of reaction. After that, the acid suspension was dialyzed using the membrane until the dialyzed water became colorless. PANI was doped in HCl solution (1 mol/L, ~2 g PANI in 50 ml) for 3 h with magnetic stirring. Finally, PANI was separated from the HCl solution by ultra-centrifugation (20 min at 12,000 rpm), washed once with distilled water and freeze-dried to yield a green powder.

The same procedure was used to synthesize PANI coated nanocellulose (PANI-NC) fibers, but in this case the nanocellulose fiber suspension (1 g/L) was previously dispersed in the ANI solution by ultrasonication. A ratio of 9.3 g ANI/g nanocellulose particles was used during synthesis.

2.3. Characterization techniques

2.3.1. Fourier transform infrared spectroscopy (FTIR)

FTIR spectra of PANI particles and PANI-NC hybrid particles (prepared as KBr pellets) were recorded using a ThermoScientific Nicolet 6700 FTIR spectrometer in transmission mode at 32 scans with a resolution of 4 cm^{-1}.

2.3.2. Thermogravimetric analysis (TGA)

Thermogravimetric tests were performed in a TGA-50 Shimadzu Thermogravimetric Analyzer at a heating rate of 10 °C/min under nitrogen atmosphere.

2.3.3. X-ray diffraction (XRD)

XRD patterns were recorded between 2° and 60°, at a scanning rate of 1°/min by using a PANalytical X'Pert Pro diffractometer equipped with Cu Kα radiation source (λ = 0.1546 nm), operating at 40 KV and 40 mA as the applied voltage and current, respectively.

2.3.4. UV–Visible spectroscopy (UV–Vis)

UV–Visible spectra of diluted suspensions of PANI and PANI-NC fibers (10 ppm) in 0.1 mol/L aqueous HCl solution and 0.1 mol/L aqueous NaOH solution, in the wavelength range 300–1000 nm, were obtained using an Agilent UV–VIS spectrometer, model 8453.

2.3.5. Field emission scanning electron microscopy (FESEM)

The surface morphology of PANI and PANI-NC fibers films was investigated using a field emission scanning electron microscope (Zeiss, model Leo 982 Gemini) at 3 kV. Sample specimens were prepared by depositing a very diluted drop of filler suspension in water onto a FTO glass, followed by spreading with nitrogen flow and finally drying at room conditions.

2.3.6. Transmission electron microscopy (TEM)

Internal morphology of PANI-NC particles was analyzed using a transmission electron microscope (Philips CM 200 UT, with ultra-twin lens for high resolution images) at 200 keV, using a dilute aqueous dispersion of particles deposited onto carbon grids.

2.3.7. Rheological tests

The complex viscosity curves of diluted fiber suspensions (3 wt%) as a function of the angular frequency were obtained using an Anton Paar, Physica MCR rheometer. Frequency sweeps from 0.1 to 500 s^{-1} using cone and plate geometry (25 mm diameter) were performed at 25 °C. The applied deformation was kept at 10%.

2.3.8. Electrical properties

A Keithley 199 System DMM/Scanner multimeter was used to measure the DC electrical conductivity on PANI and PANI hybrids pellets. The multimeter automatically calculates resistance in the four-point probe configuration. Conductivity was calculated using the relationship:

$$\sigma = \frac{L}{RA}$$

where R is the resistance of the pellet calculated by the instrument, A the electrode surface, and L the electrode spacing (about 1.7 mm in this work). The pellets were prepared using about 0.6 g of particles, applying a pressure of 5 ton/m^2 and then were gold sputtered.

3. Results and discussion

3.1. Physical and thermal characterization

In this work, the sonochemical method was selected based on previous results reported in the literature [10,22]. In summary, Jing et al. demonstrated that at the early stage of polymerization, the polymers formed by both methods, mechanical stirring and ultrasonication, take the form of nanofibers. However, as the reaction progresses, these primary nanofibers grow and agglomerate into irregular shaped PANI particles in the mechanically stirred system, while in the case of the ultrasonic irradiation, the growth and agglomeration are effectively prevented, preserving thus the PANI nanofibers in the final product. Since avoiding secondary growth and particle agglomeration is one of the main goals of this paper, the selection of the synthesis by the sonochemical method was obvious.

On the other hand, and according to Stejskal et al. [3], colloidal PANI nanoparticles are produced by the polymerization of aniline in the presence of suitable water-soluble polymers or nanoparticulate stabilizers, as in the present case when we included nanocellulose in the reaction media. However, we found that both of the nanoparticles obtained after the freeze–drying step (green colored powders) could be re-dispersed easily in water and polar solvents like as MIBK [6] and DMF [23] by ultrasonication (1 h), leading to green colored suspensions that remain stable and translucent for 280 min (PANI) or 295 min (PANI-NC), as shown in Fig. 1. After that period, a clear particle agglomeration took place, followed by sedimentation.

The FTIR spectra of the PANI and PANI-NC doped nanostructures are shown in Fig. 2 and revealed the presence of all of the characteristic absorption bands expected for the polyaniline: the band at 3220–3225 cm^{-1} is the result of different types of intra- and intermolecular hydrogen-bonded N–H stretching vibration and indicate that these PANI structures are highly hydrogen bonded [2,24]; the signals at 1562 and 1483 cm^{-1} correspond to the C=C stretching modes of the quinonoid rings and benzenoid rings in the polyaniline chain, respectively [2,25] and confirm that the structures are doped (i.e. after HCl doping, the bands at 1587 and 1494 cm^{-1} undergo a shift of about 20–30 cm^{-1} to lower wavenumbers, as indicated by Kebiche et al. [9]). Moreover, the quinonoid band at 1562 cm^{-1} has a visible shoulder at

Fig. 1. Colloidal dispersions of PANI and PANI-NC in water (50 ppm).

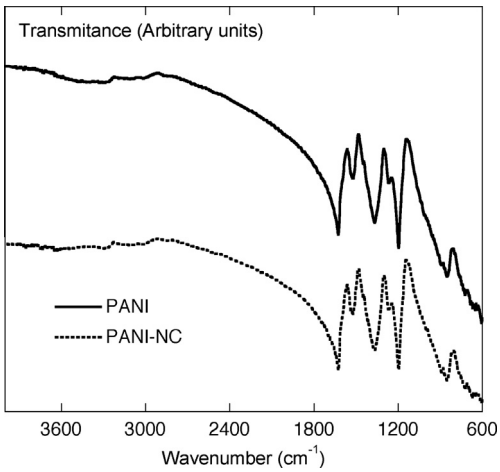

Fig. 2. FTIR spectra of PANI and PANI-NC particles.

1612 cm^{-1}, which is more noticeable in the PANI-NC spectrum than in that corresponding to PANI particles, attributed to a Raman-active —C=C— ring-stretching vibration which becomes infrared-active when the protonation induces conformational changes in the polymer chain [26]. The peak at 1302 cm^{-1} is the result of the stretching vibrations of C–N [2,25,27] while the band characteristic of the conducting protonated form is observed at 1244–1250 cm^{-1} and interpreted as a C–N+· stretching vibration in the polaron structure [28]. The 1140–1144 cm^{-1} band is assigned to a vibration mode of the –NH+= structure, which is formed during protonation [28]. Moreover, the band at about 1142 cm^{-1}, has been used by Chiang and MacDiarmid [12,29] as a measure of the extent of electron delocalization in the polymer, thus, the intensity of this peak is, therefore, to be considered as a measure of the degree of doping of the polymer backbone [12,28,29]. The region 900–700 cm^{-1} corresponds to the aromatic ring and out-of-plane deformation vibrations [12,25,26]. As can be noticed, no important differences are found in both spectra, which means that no additional peaks, attributed exclusively to the cellulose, are noticed in spectrum of the PANI-NC particles. This observation was explained by three main factors [6]: (i) the low concentration of cellulose in the hybrid sample (9.71 wt% respect to the total weight of ANI + cellulose), (ii) the fact that cellulose fibers are expected to be completely coated by PANI and (iii) the fact that the intensity of the signals coming from the polyaniline are much more stronger than those expected from the NC, which is probably the result of the electromagnetic shielding of the PANI to the NC core. This "masking effect" was also noticed and tried to explain in other works. For example, Langkammer [30] presented the same conclusions in the discussion of the FTIR spectra obtained from nanocellulose and PANI/nanocellulose sheets. He indicated that even the most noticeable peak of the nanocellulose (O–H stretching vibration) could not be observed in the PANI/nanocellulose spectrum due to the large amount of PANI that was deposited on the cellulose sheet, making the OH groups almost invisible because the nanofibers were fully covered by the polymer. Another example can be found in the paper of Mo and coworkers [31], who prepared cellulose/PANI composites, and examined them by FTIR. They presented the spectrum of the composite sample containing 11.5% PANI and 88.5% nanocellulose and compared it with those of neat PANI and neat cellulose. They observed that the relative intensity around the 3431 cm^{-1} band of the composite is much weaker than expected.

Fig. 3 shows the TGA curves of the PANI and PANI-NC nanostructures. The curve for the PANI particles has three weight loss stages. The first stage from room temperature to 150 °C is

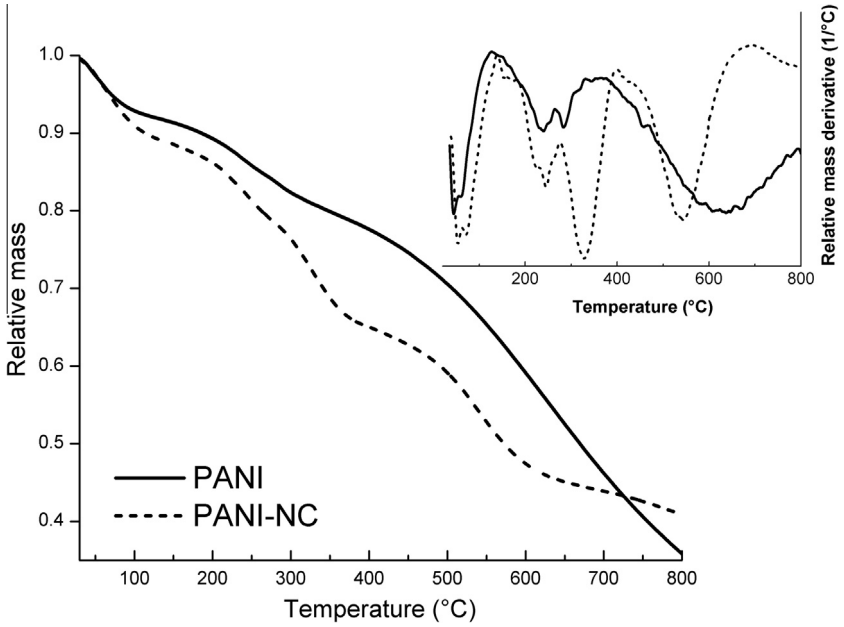

Fig. 3. Thermogravimetric curves of PANI and PANI-NC structures. Inset: derivative curves of PANI and PANI-NC particles.

attributed to the release of the moisture. The second stage between 250 and 350 °C is caused by the dedoping and a gradual decomposition initiated by dopants. The third stage arises from rapid thermal degradation of the main PANI chains. The thermal decomposition pattern of the PANI nanofibers is very similar to those of conventional PANI previously reported [5,25,32]. However, the degradation pattern of PANI-NC structures is more complex and at least four stages can be identified. The onset decomposition temperatures of the two first steps are slightly increased (from 51.5 to 61.5 °C and from 230 to 244 °C) for the hybrid structures probably due to the increased crystallinity of PANI-NC respect to neat PANI fibers, since the cellulose core is highly crystalline. It would need more energy for the water/acid to be removed from the polymer chains if they are well arranged in a more crystalline structure, as reported by Zhang et al. [5]. Thus, the second weight loss stage of PANI-NC, shifted to higher temperature, overlap with the third weight loss stage, with maximum degradation rate at 330 °C, which was identified as the thermal degradation of cellulose [33]. However, it is noticed that the last degradation step of the hybrid PANI fibers, attributed to the degradation of PANI backbone, exhibited its maximum degradation rate at lower temperature (545 °C vs. 633 °C) than in the neat PANI structures, which clearly indicates that there are interactions between both constituents of the composite fibers that affect its thermal degradation pattern. Similar results were reported by Nyström et al. [34] for polypyrrole-microfibrillated cellulose composites.

XRD was used to further characterize the structure of the PANI and cellulose covered PANI nanoparticles, as shown in Fig. 4. Five peaks centered at $2\theta = 6.5°$, 9°, 15°, 20°, and 25° are observed for the neat PANI microstructures. These peaks are in fact superimposed on a broad scattering centered at ca. $2\theta \sim 25°$, which is associated with X-ray diffraction of amorphous regions in the sample [35]. Similar to the PANI prepared by conventional methods [2,36], the peaks centered at $2\theta = 20°$ and 25° are ascribed to the periodicity parallel and perpendicular to the polymer chains of PANI, respectively, and indicates that PANI is partially crystalline as previously reported [37]. The newly appeared sharp peak centered at $2\theta = 6.5°$ corresponds to the periodicity distance between the dopant and the N atom on adjacent main chains which indicates the ordering of the dopant molecules in tunnels between

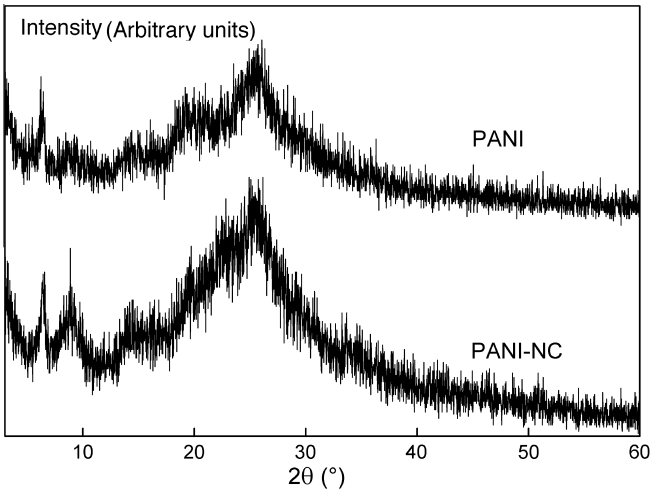

Fig. 4. X-ray diffraction patterns of PANI and PANI-NC particles.

the PANI chains [2,38] and it is attributed to the formation of highly crystalline materials [37]. These results suggest that this PANI microstructure has a better crystallinity than that of conventional PANI. The small peak at ca. $2\theta \sim 9°$ as well the one at $2\theta \sim 15°$, have been attributed to class I emeraldine salt doped with HCl, which is in general formed when the polymer is obtained from solution in the protonated form [35]. Moreover, the main reflections observed in the PANI diffraction pattern can be indexed in a pseudoorthorhombic cell with lattice parameters $a = 4.3$ Å, $b = 5.9$ Å, $c = 9.6$ Å, and $V = 245$ Å^3 [35].

On the other hand, the PANI-NC particles present a similar diffractogram, being the main differences the higher intensity of the $2\theta \sim 9°$ peak and the appearance of a new one at $2\theta \sim 22.5°$, which is corresponding to the most intense peak observed in the neat nanocellulose diffraction pattern [39].

The UV–Vis absorption spectra of PANI and PANI-NC dispersions (10 ppm) in aqueous HCl and NaOH (0.1 mol/L) solutions obtained to study the doped and dedoped forms, respectively, are shown in Fig. 5. These spectra show that dedoped PANI and

PANI-NC fibers exhibit two absorption bands: the first one in the 330–350 nm range (Band I), attributed to the electronic transition $\pi-\pi^*$ in the benzenoid rings [36] and the second one in the 610–690 nm zone (Band II), corresponding to a benzenoid to quinoid excitonic transition. [10]. The spectra are attributed to the formation of the emeraldine base, as reported in related papers [16,40]. It is clearly seen that PANI-NC bands are centered at lower wavelengths and have different relative intensity than neat PANI ones. In fact, the hypsochromic shift of the first band reflects the difference in extent of π-conjugation [41] while the second one plays an important role in switching polyaniline from an electric insulator to a conductor upon doping [41]. Furthermore, the intensity ratio of band I to band II (I_1/I_2) is related to the relative amount of quinoid diimine unit in polyaniline (i.e. the higher oxidation state of polyaniline the lower the I_1/I_2 ratio) [41]. Therefore, the relatively higher I_1/I_2 ratio exhibited by the PANI-NC nanostructures indicates that they are in a lower oxidation state than neat PANI particles. Moreover, the decreased extent of π-conjugation of the hybrid particles respect to neat PANI ones could be attributed to an increased phenyl ring torsion angle, which would result form steric repulsion due to the presence of nanocellulose in the reaction media [42] or possibly to the graphitic ordering exhibited by the PANI-NC particles, which is discussed in the following section.

On the other hand, in the spectra of the doped PANI based particles two distinct bands can be noticed at 420–430 and 850–870 nm, which are attributed to polaron–π^* transition and π–polaron transition [36,43], respectively. Furthermore, the peak around 860 nm is assigned to the presence of polaron resulting from the doping process [36,44]. The spectra are slightly different in intensity of absorption. The more intensive absorption of neat PANI particles indicates that it has a more compact and regular microstructure than that of PANI-NC, hence, the conjugated degree of PANI microstructures is greater than that of PANI-NC [36,45]. Moreover, compared with neat PANI structures, the small blue shift of these bands from 434 to 424 nm and 867 to 849 nm indicates a slight reduction of the conjugated length in the hybrid PANI-NC particles. Additionally, the existence of only one absorption peak at 420–430 nm, as opposite as the coexistence of two different bands at about 300 and 450 nm reported in other papers [2,36,46], and the "free carrier tail" in the IR region for both samples are consistent with an expanded coil-like conformation and a delocalized polaron structure (longer conjugation length), although the delocalization is not complete [47,48]. Expanded coil makes it possible for the molecule to become coplanar, which allows the p-electrons to delocalize easily. The delocalization is responsible for the creation of the polaron structure of polyaniline and thus, leads to a significant increase of conductivity [48].

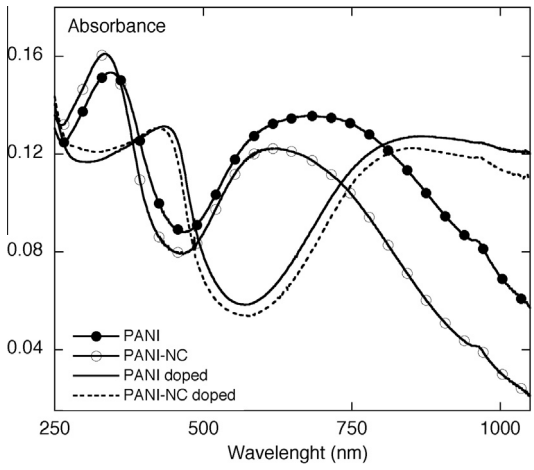

Fig. 5. UV–Vis absorption spectra of PANI and PANI-NC particles in aqueous solutions of NaOH (dedoped) and HCl (doped).

3.2. Electronic microscopy characterization

Fig. 6 shows the FESEM images of PANI and PANI-NC fibers. Particles of PANI produced by techniques of oxidative aniline polymerization in an inorganic acid water solution have a high surface tension, resulting in their tendency to aggregate, and a low specific surface, as indicated by other researchers [49]. Therefore, large aggregates of PANI particles are formed, with sizes up to several microns, as can be noticed from FESEM pictures. As it is reported elsewhere [50,51,5] the basic units formed during oxidative chemical polymerization of PANI are nanofibers but with the progress of the polymerization, the formed nanofiber will serve as scaffolds for the further growth of PANI and finally develop to a particle form. Although the sonochemical polymerization of aniline has been reported as a very good way to diminish the secondary growth [10,22], aggregation was still important in the present case. In addition, it has correctly been concluded [3,52] that this common fused morphology is produced directly during the synthesis and is not the result of mutual attraction of already formed particles. On the other hand, other authors found microstructures similar to those reported here by preparing PANI under ultrasonication: Zhang et al. [5] indicated that their particles are also in the nanoscale level, but, instead of a nanofiber structure, spherical shape was observed, and the small nanoparticles tend to agglomerate and form large arrangements.

In the present case, however, important differences between the aggregates formed by PANI-NC or neat PANI particles are noticed: the former seems to be formed by longer individual fibers while the PANI ones resemble more closely arrangements of short cylinders. Moreover, deeper observations performed by TEM on single PANI-NC fibers (Fig. 7) indicated that these structures are formed by a cellulose fiber core of about 20 nm in diameter with the polyaniline grown around it in a quite ordered shell of about 40 nm. This kind of structures was already reported for silver based fibers: in Ag_2Te–polyaniline systems [15] it was found that nanoparticles (~80–100 nm) have core–shell structure, being the particles at the core crystalline α-Ag_2Te and the shell amorphous PANI. Silver nanowires coated with PANI were also prepared and characterized by microscopy. Moreover, more recently Gu and Huang [53] deposited thin PANI film coatings onto cellulose filter paper in order to further produce nanographite sheets. These authors indicated accurately that cellulose is composed of β-D-(1-4)-glucopyranose molecular chains containing sufficient hydroxyl groups, which form inter- and intramolecular hydrogen bonds, leading to the formation of a multitude of crystalline domains in cellulose fibers. Among them, the cellulose I type commonly exists in native cellulose substances and consisted of triclinic (I_α) and monoclinic (I_β) unit cells [54]. The similarity of the molecular structures between glucopyranose and aniline led to a regular packing of PANI chains along the cellulose I_α crystalline domains [53], which is perfectly coherent with our observations: layers of ordered polyaniline can be seen on the surface of the NC, becoming disordered away from the surface.

On the other hand, sporadic star-like PANI nanostructures of around 1 μm in diagonal length were also observed (Fig. 6c and d), although the synthesis conditions do not correspond to those reported by Rezaei et al. [2] (i.e. rapid initiated strategy with glycine as dopant) or Jin and co-workers [55] (i.e. high temperature and high pressure hydrothermal conditions, using aspartic acid as dopant). Conversely, when HCl was used as dopant, the predominant form adopted by PANI was that of fibers with interconnected network structures, as indicated in related papers [2].

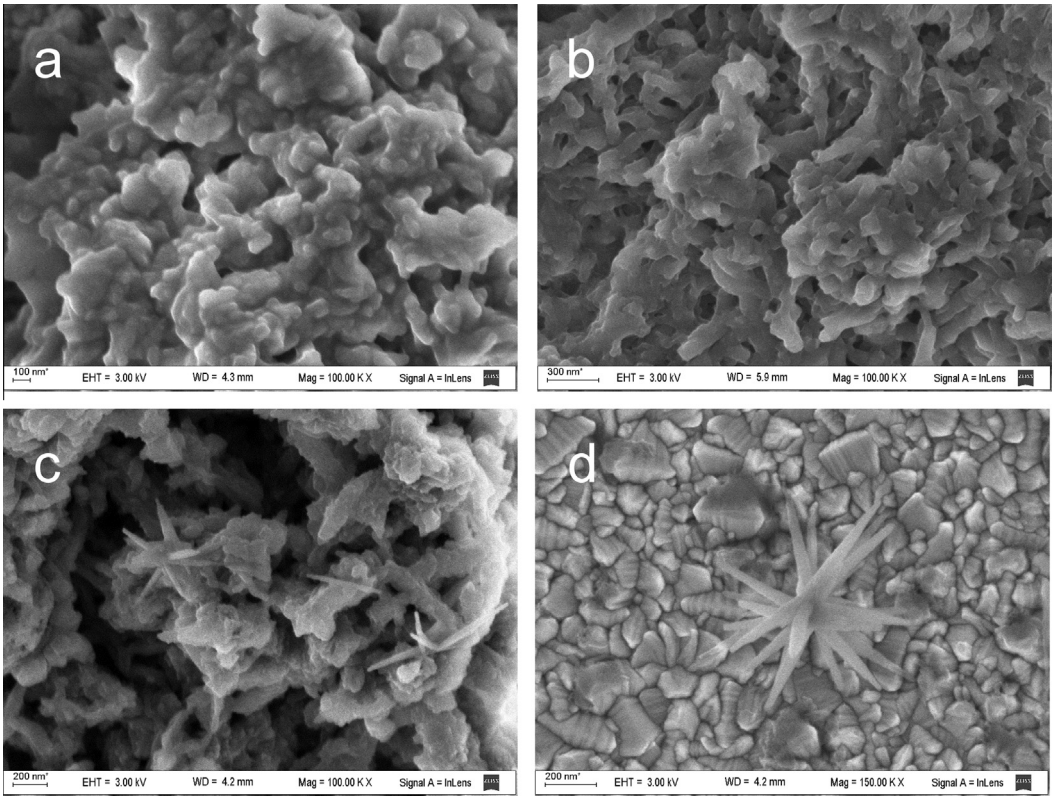

Fig. 6. FESEM images PANI based particles. (a) PANI; (b) PANI-NC; (c, d) star-like PANI nanostructures.

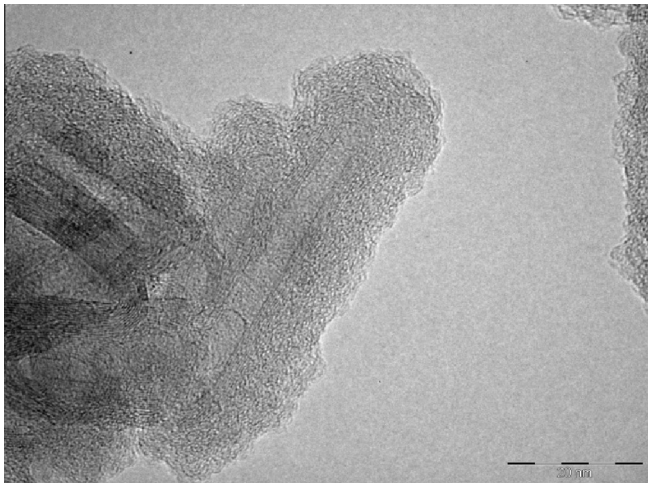

Fig. 7. TEM image of PANI-NC fibers.

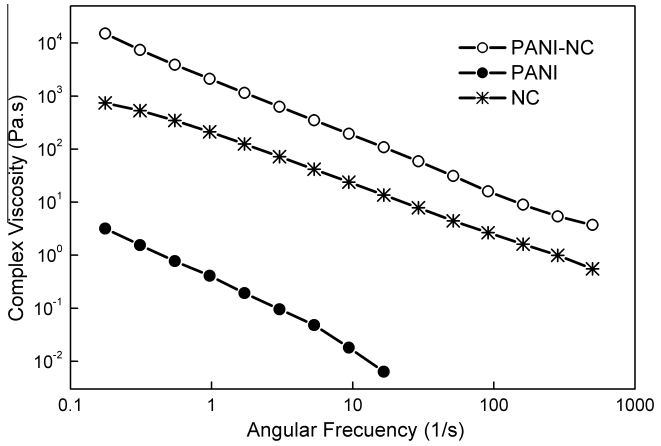

Fig. 8. Complex viscosity as a function of the angular frequency for 3 wt% aqueous suspensions of PANI, PANI-NC and NC fibers.

3.3. Suspension rheologic behavior

The morphology of both conductive particles was further investigated using rheology measurements performed on aqueous suspensions. Fig. 8 shows the complex viscosity of suspensions containing 3 wt% of PANI, PANI-NC or nanocellulose fibers as a function of the frequency. It is clear that the complex viscosity of the suspensions decreases as the angular frequency increases, resulting in a power law behavior that extended over the entire range of frequencies studied due to the alignment of the particulate structures under flow. This rheological behavior is not new in the particle suspensions literature [18,56,57] and thus, it was expected. What is surprising is the important separation between the curves corresponding to PANI-NC and nanocellulose and the neat PANI one, which could be related with the different morphology of the particles. Many simple models for describing the viscosity of particle suspensions have been derived from Einstein equation. They only consider the volume concentration of the particles, and their aspect ratio for the case of non-spherical particles [18,57]. Although in this case the densities of the particles are quite different (i.e. 1500 kg/m^3 for nanocellulose; 1000 kg/m^3 for PANI based ones), the difference in volume fraction is not enough to explain the observed behavior therefore it is attributed to the different morphology/aspect ratio added to differences in particle–particle and particle–water interaction levels.

3.4. Electrical properties

The electric conductivity of the doped PANI structure, determined from DC measurements, was determined as 0.059 S/cm, while that of the PANI-NC hybrid fibers was 0.075 S/cm, showing an increase of about 27%. This phenomenon is most likely due to the length of the nanofibers, as indicated in related papers [36]. The longer fibers will be more advantageous than the irregularly shaped nanoparticulates and aggregations for electrical applications. Since the longer ones have less contact points in the same unit distance, electrical conductivity with the longer fibers will be higher than that of the particles and aggregation [36]. Recently, Lissarrague et al. [12] confirmed the importance of the spatial distribution fluctuations of polymer chains, as a consequence of the different PANI chains arrangements due to the filler presence, on the electrical behavior of hybrid particles, by studying the effects of different nucleating particles (aluminum powder, carbon nanotubes and quartz dust) on aniline polymerization. Moreover, other researchers indicate similar behavior when comparing the electrical behavior of neat conductive polymers with that of the composite structures based on them: Sahoo et al. [58] noticed the same effect by comparing the results obtained in composites based on shape memory PU and carbon nanotubes (MWCNT) or polypyrrole coated MWCNT, indicating that the enhancement in electrical conductivity is due to the connection of the nanotubes with numerous polypyrrole domains coated onto them. Li et al. [21] prepared PANI-coated conductive paper by in situ polymerization of aniline and confirmed that the bond between PANI and cellulose existed in the form of hydrogen bonding. Moreover, they indicated that the pulp fibers promoted the dispersion of PANI particles generated, preventing their aggregation in the reaction system, which was favorable for the doping of PANI with *p*-toluenesulfonic acid. Therefore, they noticed a higher doping level of the PANI in the PANI/cellulose samples than the corresponding to neat PANI particles, which was attributed to the interaction cellulose-PANI. This last explanation can be directly applied to our system, due to the manifest similarities. On the other hand, these electric measurements confirm the success of the synthesis of conductive PANI and PANI-NC particles.

4. Conclusions

PANI-NC hybrid particles were successfully synthesized by a sonochemical method. FITR spectroscopic studies revealed that the structure of these particles in the infrared region closely resemble that of the neat PANI fibers synthesized using the same methodology. However, X-ray measurements revealed the presence of cellulose in the hybrid structures by the appearance of new peak at $2\theta \sim 22.5°$, attributed to the cellulose nanoparticles. UV–Vis curves obtained from aqueous suspensions revealed that PANI-NC particles were in a lower oxidation state than neat PANI particles while the conjugated degree of PANI microstructures resulted greater than that of PANI-NC. Microscopy investigations showed that aggregates formed by PANI-NC particles were formed by longer individual fibers while those corresponding to the neat PANI structures closely resemble arrangements of short cylinders. Moreover, TEM observations revealed that PANI-NC structures were formed by a cellulose nanofiber core with the polyaniline grown around it, forming a layered ordered shell close to the NC surface that become disordered away from the surface. The rheology of very diluted aqueous suspensions of both nanostructures was really different, which was attributed to the different morphology/aspect ratio, in addition to the differences in particle–particle and particle–water interaction levels. Moreover, the electrical conductivity of PANI-NC fibers resulted higher than that of the neat PANI fibers, which was explained taking into account the cellulose–PANI interactions developed during synthesis.

Acknowledgements

The authors thank for the financial support to National Research Council of Republic Argentina (CONICET), the Science and Technology National Promotion Agency (ANPCyT) and the National University of Mar del Plata (UNMdP).

References

[1] I.F. Perepichka, D.F. Perepichka, H. Meng, F. Wudl, Light-emitting polythiophenes, Adv. Mater. 17 (2005) 2281–2305.
[2] S.J.T. Rezaei, Y. Bide, M.R. Nabid, A new approach for the synthesis of polyaniline microstructures with a unique tetragonal star-like morphology, Synth. Met. 161 (2011) 1414–1419.
[3] J. Stejskal, I. Sapurina, M. Trchová, Polyaniline nanostructures and the role of aniline oligomers in their formation, Prog. Polym. Sci. 35 (2010) 1420–1481.
[4] R. Sainz, A.M. Benito, M.T. Martínez, J.F. Galindo, J. Sotres, A.M. Baró, et al., A soluble and highly functional polyaniline–carbon nanotube composite, Nanotechnology 16 (2005) S150–S154.
[5] X. Zhang, J. Zhu, N. Haldolaarachchige, J. Ryu, D.P. Young, S. Wei, et al., Synthetic process engineered polyaniline nanostructures with tunable morphology and physical properties, Polymer 53 (2012) 2109–2120.
[6] U.M. Casado, R.M. Quintanilla, M.I. Aranguren, N.E. Marcovich, Composite films based on shape memory polyurethanes and nanostructured polyaniline or cellulose–polyaniline particles, Synth. Met. 162 (2012) 1654–1664.
[7] R.S. Kohlman, A. Zibold, D.B. Tanner, G.G. Ihas, T. Ishiguro, Y.G. Min, et al., Limits for metallic conductivity in conducting polymers, Phys. Rev. Lett. 78 (1997) 3915–3918.
[8] B. Shedd, C.O. Baker, M.J. Heller, R.B. Kaner, H.T. Hahn, Fabrication of monolithic microstructures from polyaniline nanofibers, Mater. Sci. Eng., B 162 (2009) 111–115.
[9] H. Kebiche, D. Debarnot, A. Merzouki, F. Poncin-Epaillard, N. Haddaoui, Relationship between ammonia sensing properties of polyaniline nanostructures and their deposition and synthesis methods, Anal. Chim. Acta 737 (2012) 64–71.
[10] X. Jing, Y. Wang, D. Wu, J. Qiang, Sonochemical synthesis of polyaniline nanofibers, Ultrason. Sonochem. 14 (2007) 75–80.
[11] S. Bhadra, D. Khastgir, In situ preparation of polyaniline coated fumed and precipitated silica fillers and their composites with nitrile rubber (investigation on structure–property relationship), Eur. Polym. J. 43 (2007) 4332–4343.
[12] M.H. Lissarrague, M.E. Lamanna, N.B. D'Accorso, S. Goyanes, Effects of different nucleating particles on aniline polymerization, Synth. Met. 162 (2012) 1052–1058.
[13] H. Anno, K. Yamaguchi, T. Nakabayashi, H. Kurokawa, F. Akagi, M. Hojo, et al., Thermoelectric properties of conducting polyaniline/$BaTiO_3$ nanoparticle composite films IOP conference series, Mater. Sci. Eng. 18 (2011) 142003.
[14] L. Geng, Y. Zhao, X. Huang, S. Wang, S. Zhang, S. Wu, Characterization and gas sensitivity study of polyaniline/SnO_2 hybrid material prepared by hydrothermal route, Sens. Actuators, B 120 (2007) 568–572.
[15] Y.Y. Wang, K.F. Cai, J.L. Yin, Y. Du, X. Yao, One-pot fabrication and thermoelectric properties of Ag2Te–polyaniline core–shell nanostructures, Mater. Chem. Phys. 133 (2012) 808–812.
[16] N.V. Blinova, J. Stejskal, M. Trchová, I. Sapurina, G. Ćirić-Marjanović, The oxidation of aniline with silver nitrate to polyaniline–silver composites, Polym. Int. 50 (2009) 50–56.
[17] N.V. Blinova, P. Bober, J. Hromádková, M. Trchová, J. Stejskal, J. Prokeš, Polyaniline–silver composites prepared by the oxidation of aniline with silver nitrate in acetic acid solutions, Polym. Int. 59 (2010) 437–446.
[18] N.E. Marcovich, M.L. Auad, N.E. Bellesi, S.R. Nutt, M.I. Aranguren, Cellulose micro/nanocrystals reinforced polyurethane, J. Mater. Res. 21 (2006) 870–881.
[19] O. van den Berg, M. Schroeter, J.R. Capadona, C. Weder, Nanocomposites based on cellulose whiskers and (semi)conducting conjugated polymers, J. Mater. Chem. 17 (2007) 2746–2753.
[20] L.H.C. Mattoso, E.S. Medeiros, D.A. Baker, J. Avloni, D.F. Wood, W.J. Orts, Electrically conductive nanocomposites made from cellulose nanofibrils and polyaniline, J. Nanosci. Nanotechnol. 9 (2009) 2917–2922.
[21] J. Li, X. Qian, L. Wang, X. An, XPS characterization and percolation behavior of polyaniline-coated conductive paper, Bioresources 5 (2010) 712–726.
[22] X. Jing, Y. Wang, D. Wu, L. She, Y. Guo, Polyaniline nanofibers prepared with ultrasonic irradiation, J. Polym. Sci., Part A: Polym. Chem. 44 (2006) 1014–1019.
[23] U.M. Casado, N.E. Marcovich, M.S. Castro, M.I. Aranguren, Transparent Films Based on Polyaniline and Cellulose Nanofibers, in: Proceedings ArChiPol´09, Los Cocos, Cordoba, Argentina, 2009, pp. 274–275.
[24] E. Marie, R. Rothe, M. Antonietti, K. Landfester, Synthesis of polyaniline particles via inverse and direct miniemulsion, Macromolecules 36 (2003) 3967–3973.

[25] H. Yu, C. Wang, J. Zhang, H. Li, S. Liu, Y. Ran, et al., Cyclodextrin-assisted synthesis of water-dispersible polyaniline nanofibers by controlling secondary growth, Mater. Chem. Phys. 133 (2012) 459–464.
[26] I. Šeděnková, M. Trchová, J. Stejskal, Thermal degradation of polyaniline films prepared in solutions of strong and weak acids and in water – FTIR and Raman spectroscopic studies, Polym. Degrad. Stab. 93 (2008) 2147–2157.
[27] W. Zheng, M. Angelopoulos, A.J. Epstein, A.G. MacDiarmid, Concentration dependence of aggregation of polyaniline in NMP solution and properties of resulting cast films, Macromolecules 30 (1997) 7634–7637.
[28] I. Šeděnková, J. Prokeš, M. Trchová, J. Stejskal, Conformational transition in polyaniline films – spectroscopic and conductivity studies of ageing, Polym. Degrad. Stab. 93 (2008) 428–435.
[29] J.-C. Chiang, A.G. MacDiarmid, "Polyaniline": Protonic acid doping of the emeraldine form to the metallic regime, Synth. Met. 13 (1986) 193–205.
[30] J. Langkammer, In-situ Polymerization of Polyaniline on Cellulose Nanofibers: Effects on Electrical Conductivity and Tensile Properties, (2014) <http://hdl.handle.net/11299/162358>.
[31] Z.-L. Mo, Z.-L. Zhao, H. Chen, G.-P. Niu, H.-F. Shi, Heterogeneous preparation of cellulose–polyaniline conductive composites with cellulose activated by acids and its electrical properties, Carbohydr. Polym. 75 (2009) 660–664.
[32] D. Ragupathy, P. Gomathi, S.C. Lee, S.S. Al-Deyab, S.H. Lee, H.D. Ghim, One-step synthesis of electrically conductive polyaniline nanostructures by oxidative polymerization method, J. Ind. Eng. Chem. 18 (2012) 1213–1215.
[33] M.L. Auad, T. Richardson, W.J. Orts, E.S. Medeiros, L.H. Mattoso, M.A. Mosiewicki, N.E. Marcovich, M.I. Aranguren, Polyaniline modified cellulose nanofibrils as reinforcement of a smart polyurethane, Polym. Int. 60 (2011) 743–750.
[34] G. Nyström, A. Mihranyan, A. Razaq, T. Lindström, L. Nyholm, M. Strømme, Nanocellulose polypyrrole composite based on microfibrillated cellulose from wood, J. Phys. Chem. B 114 (2010) 4178–4182.
[35] J.P. Pouget, M.E. Jozefowicz, A.J. Epstein, X. Tang, A.G. MacDiarmid, X-ray structure of polyaniline, Macromolecules 24 (1991) 779–789.
[36] X. Wang, X. Wang, Y. Wu, L. Bao, H. Wang, Interfacial synthesis of polyaniline nanostructures induced by 5-sulfosalicylic acid, Mater. Lett. 64 (2010) 1865–1867.
[37] L. Zhang, M. Wan, Self-assembly of polyaniline—from nanotubes to hollow microspheres, Adv. Funct. Mater. 13 (2003) 815–820.
[38] L. Zhang, L. Zhang, M. Wan, Y. Wei, Polyaniline micro/nanofibers doped with saturation fatty acids, Synth. Met. 156 (2006) 454–458.
[39] H. Biao, T. Li-Rong, D. Da-Song, O. Wen, L. Tao, C. Xue-Rong, Preparation of Nanocellulose with Cation-Exchange Resin Catalysed Hydrolysis, in: R. Pignatello (Ed.), Biomaterials Science and Engineering, InTech, 2011.
[40] N.-R. Chiou, A.J. Epstein, A simple approach to control the growth of polyaniline nanofibers, Synth. Met. 153 (2005) 69–72.
[41] Y. Wei, K.F. Hsueh, G.W. Jang, A study of leucoemeraldine and effect of redox reactions on molecular weight of chemically prepared polyaniline, Macromolecules 27 (1994) 518–525.
[42] J. Yue, Z.H. Wang, K.R. Cromack, A.J. Epstein, A.G. MacDiarmid, Effect of sulfonic acid group on polyaniline backbone, J. Am. Chem. Soc. 113 (1991) 2665–2671.
[43] T. Abdiryim, Z. Xiao-Gang, R. Jamal, Comparative studies of solid-state synthesized polyaniline doped with inorganic acids, Mater. Chem. Phys. 90 (2005) 367–372.
[44] X. Li, C. Bian, W. Chen, J. He, Z. Wang, N. Xu, et al., Polyaniline on surface modification of diatomite: a novel way to obtain conducting diatomite fillers, Appl. Surf. Sci. 207 (2003) 378–383.
[45] S. Liu, K. Zhu, Y. Zhang, J. Xu, Cyclic polyaniline nanostructures from aqueous/organic interfacial polymerization induced by polyacrylic acid, Polymer 47 (2006) 7680–7683.
[46] T. Hino, T. Namiki, N. Kuramoto, Synthesis and characterization of novel conducting composites of polyaniline prepared in the presence of sodium dodecylsulfonate and several water soluble polymers, Synth. Met. 156 (2006) 1327–1332.
[47] Y. Xia, A.G. MacDiarmid, A.J. Epstein, Camphorsulfonic acid fully doped polyaniline emeraldine salt: in situ observation of electronic and conformational changes induced by organic vapors by an ultraviolet/visible/near-infrared spectroscopic method, Macromolecules 27 (1994) 7212–7214.
[48] J. Laska, Conformations of polyaniline in polymer blends, J. Mol. Struct. 701 (2004) 13–18.
[49] A. Pud, N. Ogurtsov, A. Korzhenko, G. Shapoval, Some aspects of preparation methods and properties of polyaniline blends and composites with organic polymers, Prog. Polym. Sci. 28 (2003) 1701–1753.
[50] J. Huang, R.B. Kaner, The intrinsic nanofibrillar morphology of polyaniline, Chem. Commun. (2006) 367–376.
[51] S. Banerjee, A. Kumar, Dielectric behavior and charge transport in polyaniline nanofiber reinforced PMMA composites, J. Phys. Chem. Solids 71 (2010) 381–388.
[52] D. Li, R.B. Kaner, Shape and aggregation control of nanoparticles: Not shaken, not stirred, J. Am. Chem. Soc. 128 (2006) 968–975.
[53] Y. Gu, J. Huang, Nanographite sheets derived from polyaniline nanocoating of cellulose nanofibers, Mater. Res. Bull. 48 (2013) 429–434.
[54] H.P.S. Abdul Khalil, A.H. Bhat, A.F. Ireana Yusra, Green composites from sustainable cellulose nanofibrils: a review, Carbohydr. Polym. 87 (2012) 963–979.
[55] E. Jin, X. Lu, X. Bian, L. Kong, W. Zhang, C. Wang, Unique tetragonal starlike polyaniline microstructure and its application in electrochemical biosensing, J. Ind. Eng. Chem. 20 (2010) 3079.
[56] M.A.S. Azizi Samir, F. Alloin, J.-Y. Sanchez, N. El Kissi, A. Dufresne, Preparation of cellulose whiskers reinforced nanocomposites from an organic medium suspension, Macromolecules 37 (2004) 1386–1393.
[57] E. Guth, Theory of filler reinforcement, J. Appl. Phys. 16 (1945) 20–25.
[58] N.G. Sahoo, Y.C. Jung, H.J. Yoo, J.W. Cho, Influence of carbon nanotubes and polypyrrole on the thermal, mechanical and electroactive shape-memory properties of polyurethane nanocomposites, Compos. Sci. Technol. 67 (2007) 1920–1929.